ChemComm

Accepted Manuscript

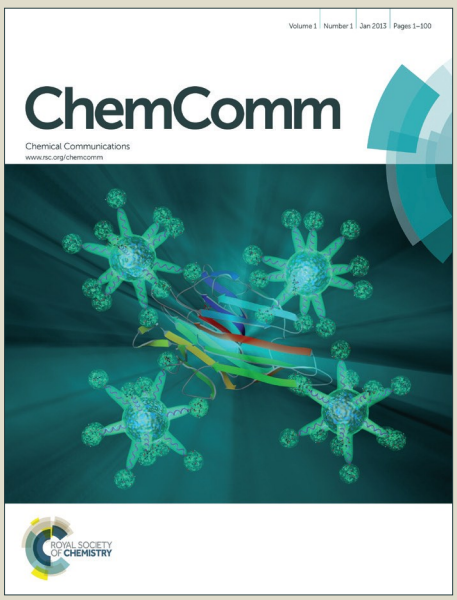

ROYAL SOCIETY OF CHEMISTRY

www.rsc.org/chemcomm

Journal Name

ARTICLE

Layered double hydroxides toward electrochemical energy storage and conversion: design, synthesis and applications

Received 00th January 20xx,
Accepted 00th January 20xx

DOI: 10.1039/x0xx00000x

www.rsc.org/

Mingfei Shao, Ruikang Zhang, Zhenhua Li, Min Wei,* David G. Evans and Xue Duan

Two-dimensional (2D) materials have attracted increasing interest in electrochemical energy storage and conversion. As a typical 2D material, layered double hydroxides (LDHs) display large potential in this area due to their facile tunability in composition, structure and morphology. Various preparation strategies, including *in situ* growth, electrodeposition and layer-by-layer (LBL) assembly, have been developed to directly modify electrodes by using LDHs materials. Moreover, several composite materials based on LDHs and conductive matrix have also been rationally designed and employed in supercapacitors, batteries and electrocatalysis with largely enhanced performances. This Feature Article summarizes the latest developments in the design, preparation and evaluation of LDHs materials toward electrochemical energy storage and conversion.

1. Introduction

With the increasing requirements of reliable and environmentally friendly energy resources, electrochemical energy storage and conversion systems (such as batteries, supercapacitors (SCs) and water splitting) have attracted intense interest in the past decades,[1–6] which promotes the discovery and optimization of new high-performance materials. Recently, two-dimensional (2D) materials have evoked extensively studies in electrochemistry due to their high specific surface area, unique structure and rich physicochemical properties. For example, owing to the superior electrical conductivity, high theoretical surface-to-mass ratio (~2600 $m^2 g^{-1}$) and flexibility, graphene illustrates a promising potential to store electric charge and ions.[7–9] Up to now, a wide variety of 2D materials have been successfully obtained with tunable intrinsic physicochemical properties, including transitional metal oxides,[10,11] carbides,[12–14] dichalcogenides[15,16] and layered double hydroxides,[17–20] which are regarded as excellent candidates for electrochemical energy storage and conversion.

Layered double hydroxides (LDHs) are typical inorganic layered materials which can be described by the general formula $[M^{II}_{1-x}M^{III}_{x}(OH)_2]^{z+}(A^{n-})_{z/n}{\cdot}yH_2O$, in which M^{II} and M^{III} are divalent (e.g., Mg^{2+}, Ni^{2+}, Co^{2+}, Zn^{2+}, or Fe^{2+}) and trivalent cations (e.g., Al^{3+}, Fe^{3+}, Cr^{3+} or Ga^{3+}), respectively; A^{n-} is the interlayer anion compensating for the positive charge of the brucite-like layers. The easy tunability of metal ions without altering the structure as well as anion exchange properties of LDHs make them an interesting alternative for applications in catalysis,[21–23] adsorption,[24,25] biology,[26,27] energy storage and conversion.[28–30] Moreover, the high dispersion of active species in a layered matrix, the facile exfoliation into monolayer nanosheets and chemical modification open new opportunities for LDHs as multifunctional electrodes. Based on the intriguing features above, progress toward LDHs-based electrodes has largely benefited from the increasing development of advanced materials with well-controlled composition (including host layers and guest molecules), tunable nanostructure (from nanoparticles to hierarchical architecture) and hybrid nanocomposite.

In this review, we will comprehensively summarize recent progress in the strategies of electrode modification by using LDHs, including *in situ* growth, electrodeposition and layer-by-layer (LBL) assembly. Subsequently, various nanostructures of LDHs (e.g., microspheres and nanoplatelets arrays) as well as their nanocomposites (e.g. LDHs/carbon and LDHs/polymer) with excellent electrochemical performances in supercapacitors, batteries and electrocatalysis will be introduced. Current challenges and future strategies are also discussed from the viewpoint of material design and practical application. It is anticipated that this Feature Article will focus more attention toward the electrochemical properties of LDH-based materials and encourage future work in this exciting area.

2. The preparation of LDHs-based electrodes

In spite of large potential in electrochemical energy storage and conversion for LDHs materials, the time- and cost-effective modification of electrodes is the first challenge to explore their fascinating electrochemical properties and broad applications. To date, a number of methods have been used for the deposition of LDHs nanoparticles on the surface of conducting

State Key Laboratory of Chemical Resource Engineering, Beijing University of Chemical Technology, Beijing 100029, China. E-mail: weimin@mail.buct.edu.cn

substrates. It is known that the pre-synthesized LDHs nanoparticles suspension can be directly introduced onto the electrode by traditional dipping or spin-coating method. However, these approaches usually lead to the aggregation of nanoparticles and thereby largely limit their electrochemical performances. In this section, we aim to briefly summarize several different routes for the fabrication of LDH-based electrodes with high disperse and ordered nanostructures by *in situ* growth, electrodeposition and LBL assembly method.

2.1. *In situ* growth

LDHs nanoplatelet arrays with direct growth on the surface of conducting substrates (conducting glasses, papers, clothes or metals) have evoked increasing interest as a result of their largely improved conductivity, efficient exposure of active sites and simplified electrode manufacturing process, in comparison with LDH powdered samples. *In situ* growth of LDHs usually results in an oriented and rigid nanoplatelets array architecture, which allows an easy access of electrolyte to the entire nanosheets and thereby improves the overall performance of LDHs-based electrodes. Liu *et al.*[31] first reported a facile synthesis of CoFe-LDH nanowall arrays (NWAs) robustly built on a flexible Fe-Co-Ni substrate through a hydrothermal method. An ultrasonication test of 30 min toward the as-made CoFe-LDH NWAs has demonstrated their ultra-robust mechanical adhesion to the substrate (Figure 1a and b). Zhang *et al.*[32] prepared thin films of NiAl-LDH on Ni foil and Ni foam substrates by secondary (seeded) growth of NiAl-LDH seed layer. The preparation procedure consists of deposition of LDH seeds from a colloidal suspension on the substrate *via* dip coating, followed by a hydrothermal treatment of the nanocrystals to form LDH film. The secondary grown film is found to provide a higher crystallinity and more uniform composition of metal cations than the *in situ* grown film on seed-free substrate under identical hydrothermal conditions. Han *et al.*[33] further demonstrated a CoAl-LDH nanoplatelet array grown on a flexible Ni foil substrate by using urea as alkali sources and NH_4F as growth assisting agent. The X-ray diffraction (XRD) patterns of the CoAl-LDH film on Ni foil and the corresponding powdered sample scraped from the film are rather different. For the LDH film on Ni substrate, the absence of [00l] reflections indicates a preferential orientation of LDH crystallites with their *ab* plane perpendicular to the substrate. Chen *et al*.[34] presented a facile one-step method of growing CoNi-LDH films with ultrathin nanosheets and porous nanostructures for supercapacitors using cetyltrimethylammonium bromide (CTAB) as assisting agent but without any adscititious alkali (urea and hexamine) sources and oxidants. They indicated that the surfactant CTAB might selectively stabilize the exposed planes of nanosheets and finally improve the size uniformity of nanosheets through electrostatic interaction between the ionic head-groups of CTAB and the OH^- groups of CoNi-LDH nanosheets. Our group[35] synthesized NiMn-LDH on carbon nanotube (CNT) backbone by the chemical modification of CNT surface with functional groups (e.g., $-OH^-$, $-CO$, $-COO^-$) (Figure 1c). It is found that the improvement of hydrophilic treatment by modification was crucial to the subsequent growth of LDH. Similarly, Lu *et al.*[36] fabricated 3D films of vertically aligned NiFe-LDH nanoplates loaded on nickel foam as electrodes for oxygen evolution reaction (OER) by a simple hydrothermal method without a growth assisting agent. As demonstrated above, the formation of LDHs crystal nucleus on the surface of substrates is a key step for the *in situ* synthesis approach, which can be achieved by directly activating metal substrate, introducing LDH seeds as well as creating molecular interaction between LDHs nucleus and the substrates.

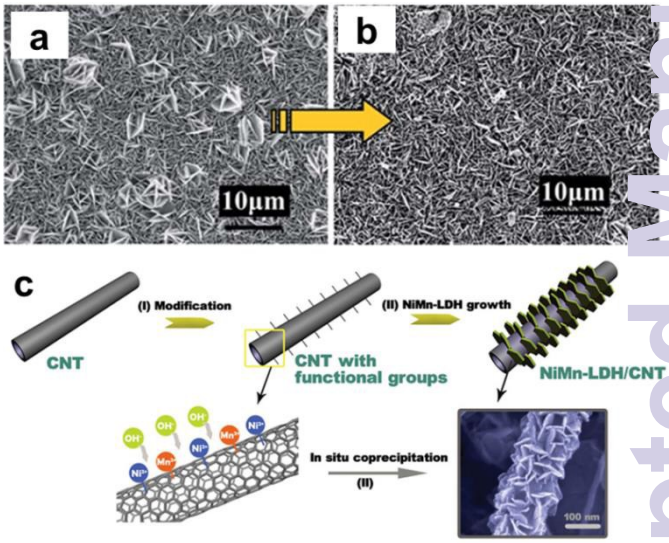

Figure 1. SEM images of (a) before and (b) after a 30 min ultra-sonication test for CoFe-LDH NWAs grafted on the Fe-Co-Ni substrate. (c) Schematic illustration for the synthesis and morphology of NiMn-LDH/CNT. Step (I): the surface modification of CNT by functional groups (e.g., $-OH^-$, $-CO$, $-COO^-$). Step (II): the grafting of NiMn-LDH nanosheets onto CNT backbone by an *in situ* growth method. Reproduced with permission from ref. 31 and 35.

2.2. Electrodeposition

The fast and facile electrochemical synthesis route has also been developed for the fabrication of LDHs electrodes.[37–46] Generally, electrodeposition was developed using nitrate or sulfate solutions containing appropriate metal ions. The deposition can be achieved by reducing nitrate or sulfate ions to generate hydroxide ions that elevate the local pH on the working electrode, resulting in the precipitation of corresponding LDHs:

$$NO_3^- + H_2O + 2e \rightarrow NO_2^- + 2OH^- \quad (1)$$

$$SO_4^{2-} + H_2O + 2e \rightarrow SO_3^{2-} + 2OH^- \quad (2)$$

The deposition potential, pH value of the plating solution, metal type and M^{2+}/M^{3+} ratio play a great role on the purity and crystallinity of the resulting LDHs materials. Dennis *et al.*[42] studied series nickel-based hydroxides by electrocoprecipitation method from metal nitrate solutions in 1989. Yarger *et al.*[43] investigated the preparation of ZnAl-LDH films by electrochemical process. It is found that the optimum deposition potential for pure and well-ordered ZnAl-LDH film was −1.65 V (*vs*. Ag/AgCl) in 4 M KCl reference electrode at room temperature, using a solution containing 12.5 mM $Zn(NO_3)_2{\cdot}6H_2O$ and 7.5 mM $Al(NO_3)_3{\cdot}9H_2O$ with pH value of

Increasing or decreasing the aluminum concentration in the plating solution results in the formation of Al- or Zn-containing impurities, respectively. Gupta *et al.*[44] reported a nanostructured CoNi-LDH onto stainless steel electrodes by the potentiostatic deposition method at −1.0 V *vs.* Ag/AgCl using various molar ratios of $Co(NO_3)_2$ and $Ni(NO_3)_2$ in distilled water. Li *et al.*[45] prepared ZnCo-LDH with zinc sulfate heptahydrate ($ZnSO_4 \cdot 7H_2O$) and cobalt (II) sulfate. In order to partially oxidize cobalt (II) to cobalt (III), H_2O_2 solution was added to the bath solution. The as-deposited ZnCo-LDH films on Ni foil were composed of highly oriented nanowalls with the *ab* plane vertical to the substrate. Furthermore, Fe-containing LDHs with different divalent metal ions have also been obtained by using electrosynthsis method (Figure 2) by our group.[46] The electrochemical synthesis is achieved by the reduction reaction occuring on the working electrode, in which the resulting OH^- leads to the precipitation of $M_xFe_{1-x}(OH)_2$. The as-synthesized $M_xFe_{1-x}(OH)_2$ material presents a light green color; after exposure in air for ~1 h, the sample color changes from green to a brownish one, indicating the occurrence of self-oxidation of Fe^{2+} to Fe^{3+}. By using this method, ultrathin MFe-LDH (M= Ni, Co and Li) nanoplatelets (200–300 nm in lateral length; 8–12 nm in thickness) perpendicular to the substrate surface are directly prepared within hundreds of seconds (<300 s) under cathodic potential (Figure 2b, c and d). Therefore, the electrosynthesis method provides a fast and effective approach for the preparation of LDHs films with controlled composition and nanostructure. Moreover, various conducting substrates can be used for the fabrication of advanced LDHs electrodes with prospective applications.

Figure 2. (a) Schematic illustration for the synthetic route of MFe-LDH (M= Co, Ni and Li) nanoarrays. SEM images of (b) NiFe-LDH, (c) CoFe-LDH and (d) LiFe-LDH nanoplatelet arrays, respectively. Reproduced with permission from ref. 46.

2.3. Layer-by-layer (LBL) assembly

LBL strategy has been effectively used to modify electrodes, since the nanometre scale control over the assembly process usually gives a high dispersion of electroactive species with uniform orientation. LDH microcrystals can be exfoliated into positively-charged 2D monolayer sheets, which are assembled alternately with various functional anions by the LBL technique.[47–51] Recently, a large number of functional electrodes have been developed through alternating assembly of positively-charged LDH nanosheets and negatively-charged species (small molecules, metal complex, macromolecules or polymers) or anionic nanoparticles (Au, CdS or graphene oxides GO). For example, the exfoliated CoAl-LDH nanosheets were assembled alternately with negatively-charged iron (III) porphyrin on ITO substrate.[52] The LBL assembly process of the multilayer films is monitored by UV–vis absorption spectra; the intensities of the absorption bands of iron (III) porphyrin correlate linearly with the bilayer number, indicating that almost equal amount of guest molecules are incorporated into the film during each cycle. Moreover, the heterogeneous film thickness can be precisely controlled with simple manipulation. To date, several LDHs/functional molecules ultrathin films have been prepared by using LBL technique, including CoAl-LDH/naphthol green B, MgAl-LDH/cobalt phthalocyanine,[53] CoAl-LDH/ruthenium(II) complex,[54] NiAl-LDH/bi-protein,[55] which display promising electrochemical activity. In addition, negatively-charged nanoparticles can also be used to assemble with LDHs-based building blocks. Dong *et al.*[56] fabricated multilayer films of CoAl-LDH nanosheets (CoAl-LDH-NS) and GO through electrostatic LBL assembly, which has demonstrated with exceptional uniformity and versatility. The resulting CoAl-LDH-NS/GO multilayer films exhibit a high specific capacitance and good cycle stability. Our group reported ZnAl-LDH/Au nanoparticles (AuNPs) ultrathin films fabricated by the LBL assembly technique.[57] The results illustrate that the obtained ZnAl-LDH/AuNPs films possess long-range order stacking in the normal direction of the substrate and a high dispersion of AuNPs on the surface of LDH nanosheets without aggregation. This guarantees their efficient electrocatalytic performance for the oxidation of glucose.

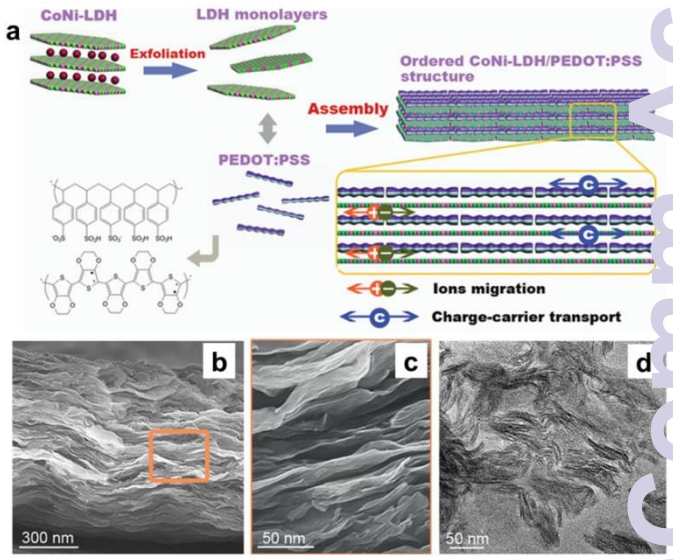

Figure 3. (a) Schematic illustration for the assembly of CoNi-LDH monolayers and PEDOT:PSS. (b, c) Cross-sectional SEM and (d) TEM image of the CoNi-LDH/PEDOT:PSS. Reproduced with permission from ref. 59

Recently, superlattice heterostructure composed of LDH monolayers and negatively-charged counterparts has been obtained by the electrostatic LBL assembly route. Yang *et al.*[58] dispersed Cl^- intercalated FeNi-LDH into a GO aqueous

suspension to obtain FeNi-LDH/GO heterostructure. The mixture was magnetically stirred for ten days to ensure the exfoliation of LDHs and the subsequent assembly of GO with FeNi-LDH nanosheets. Our group reported a molecular-scale hybrid system based on the assembly of exfoliated CoNi-LDH nanosheets and conducting polymer (poly(3,4-ethylene dioxythiophene):poly(styrene sulfonate), denoted as PEDOT:PSS) *via* an electrostatic interaction (Figure 3).[59] As shown in Figure 3b–d, the resulting LDH/PEDOT:PSS material gives a well-ordered and layer-shaped structure. This as-synthesized organic–inorganic composite with molecular-scale distribution of active species shows a largely improved capacitance and rate capability. The LDHs-based films or superlattice heterostructures obtained by the LBL self-assembly can successively inherit the intrinsic properties of both the LDHs and the counterpart; these LDHs-based film materials can be constructed by rational control over the driving force, building unit as well as the substrate.

As demonstrated above, the three methods (*in situ* growth, electrodeposition and LBL assembly) have been demonstrated as effective strategies in the preparation of LDHs-based electrodes. For the *in situ* growth method, rigid LDHs nanoplatelets arrays with tunable composition can be prepared on the surface of various substrates (e.g., conducting glass, metal sheets, carbon fibers and nanotubes); however, this method normally suffers from harsh preparation conditions, such as high temperature and time-consuming process. Alternatively, the electrodeposition method for the fabrication of LDHs electrodes effectively accelerates the preparation process even within hundreds of seconds at room temperature, with the restriction of transition metal-containing LDHs (e.g. Co, Ni, Fe, Zn) on conducting substrates. The LBL assembly method is a recently developed approach, which can achieve LDHs-based electrodes with nanometre scale control over the superlattice heterostructure, uniformity and versatility. In most cases, however, the unsatisfactory surface area of LBL film material limits their applications in large current devices, such as supercapacitors and Li-ion batteries.

3. The LDHs-based electroactive materials

LDHs materials are typical pseudocapacitive active species due to their abundant redox active sites. However, these materials often suffer from a low power performance and poor cycle life since the redox kinetics is limited by the rate of mass diffusion and electron transfer. To solve these problems, two strategies have been taken into account: (1) a well-defined micro/nanostructures with high surface area and suitable pore-size distribution is urgently needed, in which all the electroactive species participate in faradic redox reactions and a fast mass and electron transfer is guaranteed; (2) combination of LDHs with conductive matrix with improved system conductivity and electron transfer ability. Recently, some efforts have been made to improve the electrochemical performances of LDHs by creating nanostructures, and hybriding with carbon materials or conducting polymers.

3.1. The hierarchical LDHs nanostructures

Hierarchical LDHs nanostructures, especially the hollow or core–shell spheres are of great scientific and technological importance because of their specific nanostructure, high surface area and abundant mesopores.[60–62] Recently, stimulated by the promising electrochemical applications, a number of studies have been made in the synthesis of LDH microspheres by using templates or direct precipitation reactions. As an effective template, silica has been widely used to synthesize LDHs microspheres, especially hollow structures. For instance, NiAl-LDH microspheres with tunable interior architecture from core–shell to hollow structure have been obtained by LBL deposition of AlOOH on the surface of SiO_2 followed an *in situ* growth technique (Figure 4).[63] It is found that the mesopores appear gradually with the shrinking of the SiO_2 core, which thereby improves their pseudocapacitance property. Xu *et al*[64] synthesized nitrogen-enriched carbon/NiAl-LDH (N-C@LDH) hollow microspheres by using SiO_2@resorcinol-formaldehyde (RF) as a template, which gave a satisfactory electrochemical performance due to the N-doping enhanced conductivity, large specific area and favorable porous structure. In addition, LDHs spherical architectures have also been fabricated by using amorphous aluminum hydroxide (AAH) as a template.[65] Growth of such unique structure undergoes preorganization of primary nanospheres of colloidal AAH in solution, followed by the

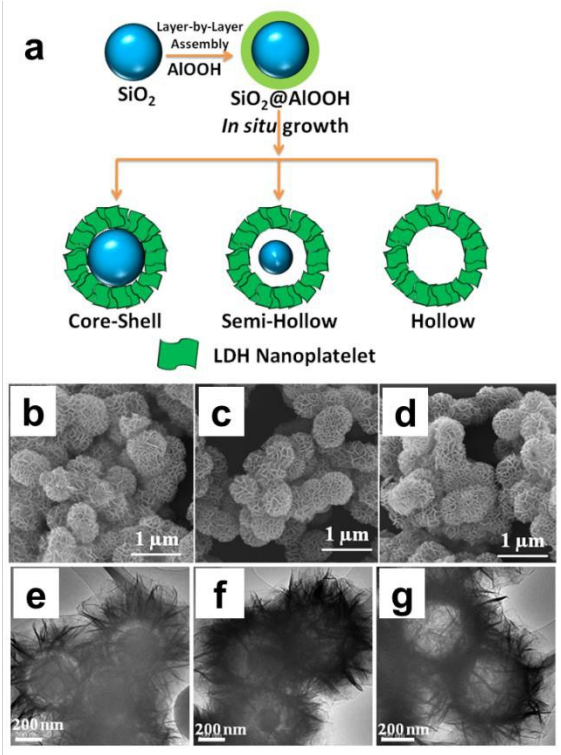

Figure 4. (a) Schemetic illustration for the preparation of LDH microspheres with tunable interior architecture from core–shell to hollow structure. SEM and TEM images of (a, e) SiO_2/NiAl-LDH core–shell microspheres; (c, f) SiO_2/NiAl-LDH yolk–shell microspheres; (d, g) NiAl-LDH hollow microsphere. Reproduced with permission from ref. 63

nucleation and crystallizaion of LDH from exterior to interior of AAH spheres *via* an *in situ* transformation mechanism. Recently, our group further demonstrated hierarchical MgFe-LDH microspheres with tunable interior structure synthesized by a surfactant-template method,[66] which displayed a three-dimensional architecture with hollow, yolk–shell and solid interior structure, respectively. Interestingly, the hollow LDH microspheres present the maximum specific surface area and the richest mesopores distribution (2–6 nm), much superior to those of yolk-shell and solid LDHs microspheres. Moreover, the hollow MgFe-LDH microspheres exhibit excellent electrocatalytic oxidation of ethanol in alkaline solution, including high activity, long-term durability and cycling stability, owing to the significantly improved faradaic redox reaction and mass transport. It is clear that the structure and morphology of LDH spheres synthesized by a hard or soft template depend on both starting raw materials and synthetic parameters including reaction time, reaction temperature, and pH value.

3.2. The LDHs-based nanocomposites

3.2.1. LDHs/carbon

Although much progress has been made, the efficiency of LDHs materials in the field of electrochemical energy storage and conversion is mainly limited by the relative sluggish charge transfer property. To solve this problem, LDHs/carbon nanocomposites with superior charge mobility and high surface area have been developed for efficient electrode materials, such as LDHs/graphene,[67–69] LDHs/CNTs[70–74] and LDHs/carbon quantum dots.[75,76] Typically, graphene with two-dimensional honeycomb-like crystal lattice shows several unique properties such as high electron mobility, large surface area, and environmental stability, which is highly desirable as a 2D catalyst support.[77] Recently, some attempts have been made to combine LDHs with graphene to enhance their electrochemical performance. Wang *et al.* synthesized a hybrid material composed of graphene nanosheets and NiAl-LDH platelets (GNS/NiAl-LDH) under mild hydrothermal conditions.[78] The NiAl-LDH platelets are homogeneously anchored onto the surfaces of GNSs as spacers to keep the neighboring sheets separate, giving rise to improved specific capacitance and stability. Graphene/CoAl-LDH hybrid composites were also fabricated by using the hydrothermal procedure, demonstrating promising electrochemical properties.[79] To further disperse LDHs nanoparticles on the surface of graphene, Zhang *et al.*[80] reported a novel NiFe-LDH/graphene hybrid prepared by means of defect-anchored nucleation and spatially confined growth of nanometer-sized NiFe LDHs into mesoporous graphene framework (Figure 5). It is found that the nitrogen dopant and topology-induced defects of graphene contribute to the adsorption and anchoring of metal cations; and the in-plane mesopores serve as nanoreactors for spatially confined nucleation and growth of NiFe-LDH. As a result, the hierarchical NiFe-LDH/graphene structure demonstrates an enhanced activity and durability for oxygen evolution under alkaline conditions.

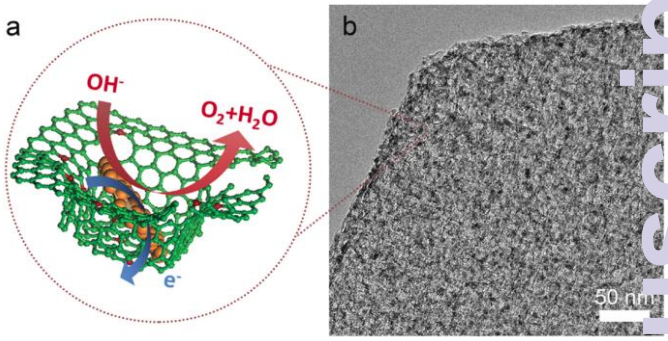

Figure 5. (a) Schematic of the spatially confined NiFe-LDH/graphene hybrids. (b) Cross sectional TEM image of a sheet of NiFe LDH/NGF electrocatalyst. Reproduced with permission from ref. 80

In addition, a sandwich-structured rGO/NiAl-LDH composite with LDH nanosheets arrays grown perpendicularly to the surface of graphene was prepared,[81] which shows a high surface area and enhanced electrochemical performance (Figure 6). The synthesis process for this hierarchical rGO/NiAl-LDH composite involves coating AlOOH colloids onto the surfaces of graphene and the subsequent *in situ* growth of NiAl-LDH nanosheet arrays *via* a hydrothermal process (Figure 6a). As shown in Figure 6b and c, the LDH nanosheet arrays are perpendicularly oriented on both sides of the graphene sheet, efficiently avoiding the stacking and aggregation of individual graphene sheets and leading to an interesting sandwich structure. The as-obtained hierarchical composite has a large specific surface area and typical mesoporous characteristics, which are favorable for achieving high pseudocapacitance performance.

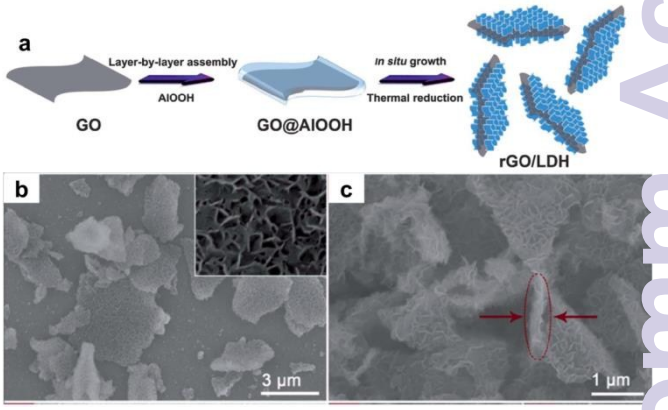

Figure 6. (a) Schematic illustration for the synthesis of rGO/NiAl–LDH composite. SEM images at different magnifications (D and E) of the hierarchical rGO/NiAl–LDH composite. Reproduced with permission from ref. 81.

Another feasible way of creating LDHs/graphene nanostructures is using the exfoliated LDHs nanosheets (LDHs-NS) as building blocks to assembly with graphene. For example, Jin *et al.*[82] demonstrated a CoAl-LDH-NS/GO composite by assembling two kinds of one-atom-thick sheets (carboxylated GO and CoAl-LDH-NS) for the pseudocapacitance application. Furthermore, assisted by the electrostatic attraction, the GO nanosheets with multifunctional oxygenic groups can be

assembled with the exfoliated NiFe-LDH sheets in aqueous solution, forming charge balancing interlayer in the resulting hybrid composite.[83] The synergy between the catalytic activity of the NiFe-LDH and the enhanced electron transport arising from graphene gives rise to superior electrocatalytic properties of the NiFe-LDH/rGO hybrid toward the oxygen evolution reaction (OER).

The exchangeable property of interlayer anions in LDHs evokes great interest on the construction of host-guest intercalation structures with desirable properties by using LDHs as host materials.[84–86] By an ion-exchange process, various organic anions have been intercalated into the interlayer space of LDHs. Carbonization under inert conditions of these intercalated LDHs gives access to a variety of interesting carbonaceous nanocomposites, which provides another effective method for the fabrication of hierarchicalnanocomposites based on LDHs and nanocarbon materials. Relative developments have been comprehensively reviewed by Zhang and Wei's group.[87] Herein, we summarized the very recently reported carbon materials synthesized by

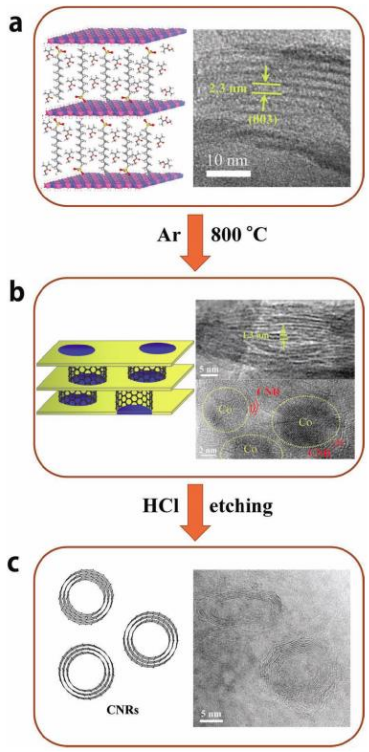

Figure 7. Schematic illustrations and HRTEM images of the different stages in the fabrication of CNRs in the CoAl-DSO-MMA-LDH matrix: (a) the CoAl-DSO-MMA-LDH precursor, (b) CoAl-DSO-MMA-LDH after calcination in an Ar atmosphere at 800 °C and (c) isolated CNRs obtained after dissolution of the matrix. Reproduced with permission from ref. 88.

using LDHs as "nanoreactors". Yang *et al.*[88] investigated a "bottom-up" synthesis of carbon nanorings (CNRs) by taking advantage of the confined space of the 2D interlayer galleries of LDH host to limit the *in situ* growth of CNRs. The CoAl-LDH containing co-intercalated dodecyl sulfonate (DSO) anions and methyl methacrylate (MMA) (CoAl-DSO-MMA-LDH) was synthesized in a one-step reaction (Figure 7a), followed by a calcination in an argon atmosphere at 800 °C. During the calcination, the thermal decomposition of LDH host is accompanied by collapse and shrinkage of the interlayer galleries, resulting in a material with a reduced interlayer spacing of ~1.3 nm (Figure 7b). It was found that Co nanoparticles embedded in the amorphous product could effectively catalyze the growth of CNRs (Figure 7c). Similar method has also been used in the confined synthesis of graphene quantum dots (GQDs). Lu *et al.*[89] obtained single-layered GQDs by the hydrothermal treatment of intercalated citrate in the confined space of MgAl-LDH gallery in the presence of ammonia at 180 °C for 8 h. The obtained solid MgAl-GQD-LDH was then etched with hydrochloric acid to produce the GQD colloidal solution.

3.2.2. LDHs/conducting polymer

Conducting polymers (CPs) such as polypyrrole (PPy), polyaniline (PANI) and poly(3,4-ethylene-dioxythiophene) (PEDOT) have attracted increasing interest for electrode materials due to their high electrical conductivity, efficient redox active sites as well as low cost.[90–92] The rational design of novel electrodes based on CPs and LDHs is highly effective

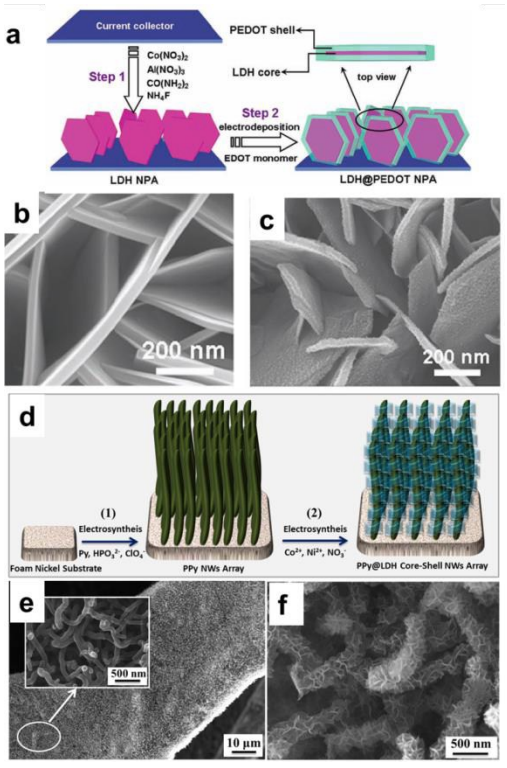

Figure 8. (a) Schematic illustration for the fabrication of LDH@PEDOT core–shell nanoplatelet array electrode. SEM images of (b) the CoAl-LDH and (c) CoAl-LDH@PEDOT NPA obtained by electrodeposition method. (d) Schematic illustration for the fabrication of PPy@LDH core–shell NWs array; SEM images of (e) PPy NWs and (f) PPy@CoNi-LDH core-shell NWs array on foam nickel substrate. Reproduced with permission from ref. 33, 97.

for achieving high performances in energy storage and conversion. It is found that the hydrophobically treated LDHs nanoparticles can be directly used to adsorb CPs. Leuteritz *et al.*[93] presented the dodecylbenzenesulfonate intercalated

MgAl-LDH based on the regeneration method, which was further modified with PANI using the solution adsorption method. Despite some agglomeration of LDH/PANI nanoparticles, a continuous phase of PANI was not observed in this composite. This highly- dispersed PANI modified LDHs gave a desirable conductivity. To obtain a more ordered structure, the exfoliated ZnAl-LDH nanosheets/PANI multilayer films on silicon wafer substrates have been fabricated by using LBL assembly method.[94] The surface of the films is microscopic smooth and uniform with a thickness of 2 nm per bilayer. In addition, CPs can be directly deposited on the surface of LDHs nanoplatelets to fabricate ordered hybrid electrode to improve the conductivity and electrochemical performances. For instance, in order to improve the conductivity of the as-grown CoAl-LDH nanoplatelet array (NPA), a thin layer of PEDOT was coated onto the surface of LDH NPA *via* potentiostatic electrodeposition method by our group (Figure 8a-c).[33] The resulting CoAl-LDH@PEDOT core–shell architecture provides a large specific surface area and excellent conductivity, which guarantees the effective redox reaction and fast electron transport between the electroactive center and current collector. Practically, CPs usually suffer from a considerable volume change during the repeated intercalation and depletion of ions in the charge and discharge process, which largely decreases their mechanical stability.[95,96] To solve this problem, we further used the PPy nanowires (NWs) as core and CoNi-LDH nanoplatelets as shell to fabricate a sophisticated nanoarray composite *via* a two-step electrosynthesis method (Figure 8d–f).[97] In view of this PPy@CoNi-LDH core–shell system, the PPy core serves as a conductive network to facilitate the electron collection and fast transport; while the LDH shell acts as a protection layer to inhibit the volumetric swelling/shrinking of PPy during long-term charge/discharge cycling.

4. The electrochemical applications

4.1. Supercapacitors

Supercapacitors (SCs) are considered as a promising candidate for next-generation power devices because of their advantages of fast charging and discharging property, high power delivery, and excellent cycling lifespan in comparison with conventional batteries and dielectric capacitors. On the basis of the charge storage mechanisms, electrochemical SCs are broadly divided into electrical double layer capacitors (EDLCs) and pseudocapacitors. In particular, pseudocapacitors entail reversible faradic redox reactions on the surface of an electro-active material for charge storage, which have a higher specific capacitance value of 10–100 times that of EDLCs.[98] Layered double hydroxides (LDHs) as a typical class of 2D structure anionic clays have been reported as excellent candidates for pseudocapacitors owing to their high theoretical specific capacity and low cost. However, LDHs materials often suffer from a low power density and cycle life because the redox kinetics is limited by the rate of mass diffusion and electron transfer. For example, CoAl-LDH nanoparticles material synthesized by traditional coprecipitation method only provides a limited specific capacitance (145 F g^{-1} at 2 A g^{-1}).[99] To solve the problem, some efforts have been made to improve the performance of LDH based SCs by creating nanostructures (such as core/shell nanowires or microfibers, nanowall films) or incorporating with conductive graphene or polymers. As demonstrated above, the core–shell LDHs microspheres with tunable interior architecture can be synthesized by using silica as hard template.[100] Interestingly, the specific capacitance of hollow NiAl-LDH microspheres reaches to 735 F g^{-1} (at 2 A g^{-1}), much larger than that of core–shell (406 F g^{-1}) and yolk–shell (524 F g^{-1}) microspheres as well as LDH nanoparticles (117 F g^{-1}). In addition, the hollow microspheres show good cycle performance (the capacitance increases 16.5% after 1000 cycles at a high charge/discharge current density of 8 A g^{-1}) and remarkable rate capability (75% capacitance is retained at a large current density of 25 A g^{-1}). The enhancement of capacitance can be attributed to the large surface area and optimal pore-size of the hierarchical hollow microspheres, which guarantees the high specific capacitance and excellent cycle stability.

Development of LDHs nanoplatelet on conductive substrate with well-defined architectures is an approach for enhancing ion and charge-carrier transport. It has been reported that CoNi-LDH arrays on nickel foam electrode display a significantly enhanced specific capacitance (2682 F g^{-1} at 3 A g^{-1}, based on active materials) and energy density (77.3 Wh kg^{-1} at 623 W kg^{-1}), as well as good stability (~82% of its original capacitance after 5000 cycles).[34] NiMn-LDH microcrystals grafted on carbon nanotube (CNT) backbone can deliver a maximum specific capacitance of 2960 F g^{-1} (at 1.5 A g^{-1}) and excellent rate capability (79.5% retention at 30 A g^{-1}).[35] CoMn-LDH growing on flexible carbon fibers (CF) *via* an *in situ* growth approach was also demonstrated by our group.[101] The resulting CoMn-LDH/CF electrode delivers a high specific capacitance (1079 F g^{-1} at 2.1 A g^{-1}) and excellent rate capability even at a rather high current density (82.5% capacitance retention at 42.0 A g^{-1}). Furthermore, a flexible solid-state supercapacitor device fabricated by using the CoMn-LDH/CFs achieves a specific energy up to 126.1 Wh kg^{-1} and a specific power of 65.6 kW kg^{-1}. Recently, the core-shell NiCo-LDH@CNT-based supercapacitor was presented with excellent performances: a maximum energy density of 89.1 Wh kg^{-1} with an operational voltage of 1.75 V, and a maximum power density of 8.7 kW kg^{-1} at an energy density of 41.7 Wh kg^{-1}.[72] Graphene, with high charge mobility and surface area, has been effectively used to support LDHs materials for efficient SCs. As a result, the NiAl-LDH/graphene composite exhibits a maximum specific capacitance of 781.5 F g^{-1} and excellent cycle life with an increased specific capacitance of 22.5% after 200 cycle tests.[78] The CoNi-LDH/rGO superlattice composites show a high specific capacitance (~500 F g^{-1}) at a discharge current up to 30 A g^{-1}, as well as excellent stability.[102] In addition, Wu et al.[69] reported a facile strategy to fabricate integrated porous CoAl hydroxide nanosheets (named as GSP-LDH) with dodecyl sulfate anions and graphene

sheets as structural and conductive supports, respectively. Owing to the fast ion/electron transport, the GSP-LDH electrode exhibits remarkably improved electrochemical characteristics, including a high specific capacitance (1043 F g^{-1} at 1 A g^{-1}), ultra-high rate performance capability (912 F g^{-1} at 20 A g^{-1}) and excellent cycling stability (~84% of the initial capacitance retention after 2000 cycles).

In addition to the carbon materials, the construction of LDHs/conducting polymer nanocomposites provides another effective route to obtain satisfactory overall supercapacitive performance, owing to the greatly improved charge transport in the electrochemical process. Recently, a molecular-scale hybrid system is constructed based on the self-assembly of CoNi-LDH monolayers and the conducting polymer (poly(3,4-ethylene dioxythiophene):poly(styrene sulfonate), denoted as PEDOT:PSS) into an alternating-layer superlattice.[59] Owing to the homogeneous interface and intimate interaction, the resulting CoNi-LDH/PEDOT:PSS hybrid materials possess a simultaneous enhancement in ion and charge-carrier transport, which exhibit improved capacitive properties with a high specific capacitance (960 F g^{-1} at 2 A g^{-1}) and excellent rate capability (83.7% retention at 30 A g^{-1}). Moreover, CoAl-LDH nanoplatelets array modified by PEDOT shows a maximum specific capacitance of 649 F g^{-1} by cyclic voltammetry (scan rate: 2 mV s^{-1}) and 672 F g^{-1} by galvanostatic discharge (1 A g^{-1}).[33] Furthermore, the hybrid CoAl-LDH@PEDOT electrode also exhibits excellent rate capability with a specific energy of 39.4 Wh kg^{-1} (40 A g^{-1}), as well as good long-term cycling stability (92.5% of its original capacitance is retained after 5000 cycles). A sophisticated nanoarray consisting of PPy core and LDHs shell *via* a two-step electrosynthesis method was presented.[97] The specific capacitance of the PPy@CoNi-LDH core–shell NWs array (2342 F g^{-1}; current density 1 A g^{-1}) is 2.1, 2.6, and 1.2 times higher than that of pristine PPy (1137 F g^{-1}), CoNi-LDH (897 F g^{-1}), and the summation of these two constitutes (2034 F g^{-1}), respectively. The specific capacitance enhancement of PPy@LDH is attributed to the synergetic effect of PPy core and LDH shell. The all-solid-state asymmetric supercapacitor device fabricated with PPy@CoNi-LDH electrode materials gives an energy density of ~46 Wh kg^{-1} (at 2.4 kW kg^{-1}), a power density of ~12 kW kg^{-1} (at 11.3 Wh kg^{-1}), and long life time (20000 cycles). Recently, LDHs-based SCs electrodes have been widely developed and the typical studies are summarized in Table 1.

4.2. Li-ion batteries

Compared with traditional lead-acid and Ni-based batteries, Li-ion batteries (LIBs) show advantages of high energy density, high operating voltage, long cycling life and environmental compatibility.[111–113] However, the demands for batteries with higher power/energy density and longer cycling life for the development of newly emerging electronic devices are still unsatisfied; the promising electrode materials as one of the key issues for the high performance of LIBs are still urgent. The wide tunability of metal ions without altering the structure of LDHs, and the transformation of LDHs into corresponding metal oxides *via* calcination make them as highly-active anode materials for LIBs. Recently, a pure $NiFe_2O_4$ spinel has been prepared from a $NiFe^{2+}Fe^{3+}$-LDHs precursor after calcination at 700 ˚C, which showed an initial discharge capacity of 1231 mAh g^{-1} and a reversible capacity of 701 mAh g^{-1}.[114] The major advantage of the LDHs precursor method for the synthesis of $NiFe_2O_4$ is that it affords a spinel with a small particle size and uniform distribution of metal cations, which facilitates the active sites exposure and the Li-ions intercalation. To enhance the performance of LDHs derived spinel, carbon coated CoFe mixed oxide nanowall arrays were evolved from thermal decomposition of CoFe-LDH precursors and carbonization of glucose.[115] The obtained carbon coated CoFe mixed oxide with improved electrical conductivity exhibits superior electrochemical performance in terms of specific capacity and cyclability compared with a carbon-free sample.

Carbon materials themselves have been widely used in LIBs because of their high surface area, extraordinary electronic and mechanical properties and low cost. However, how to obtain the highly dispersed and ordered carbon materials with improved performance for LIBs is still a challenge. Recently, it was found that LDHs can be effectively used to direct the growth of carbon materials with controlled nanostructures. As a typical example, metal oxide nanoflakes derived from LDHs precursor were employed as the template for the epitaxial growth of unstacked graphene *via* chemical vapour deposition.[116] The unstacked graphene was used for high-power lithium–sulphur batteries with excellent high-rate performance due to the fast charge/discharge process.

Similarly, graphene microspheres (GMSs) with hierarchical porous architectures were further obtained by using calcined LDH microspheres as templates, which was employed as carbon scaffold to accommodate sulfur for rechargeable lithium–sulfur batteries.[117] As a result, an initial areal discharge capacity of 2.67 mAh cm^{-2} was obtained at a current density of 0.83 mA cm^{-2} on flexible GMS paper electrode with areal sulfur loading of 2.5 mg cm^{-2}. In addition, a facile method to fabricate carbon nanorings (CNRs) *via* catalytic growth in the confined space of LDHs was also developed.[118] The CNR electrode shows a reversible specific capacity of 1263 mAh g^{-1} after 100 cycles and the coulombic efficiency increases to nearly 100%. The specific capacities are 1216, 939, 758 and 508 mAh g^{-1} at current densities of 1, 4.8, 15 and 45 A g^{-1}, corresponding to capacity retention ratios of 98%, 76%, 61% and 41%, respectively.

As discussed above, the LDHs derived metal oxides/spinel and carbon materials synthesized by using confined space of LDHs have demonstrated large potential for the advanced Li-ion batteries. The specific layered structure, tunable metal ions and intercalation property give LDHs a good chance to directly accommodate metal ions. Unfortunately, the LDHs themselves used as electro-active materials to store cations for efficient energy storage devices have not been effectively investigated until now.

4.3. Electrochemical catalysis

Water splitting by direct electrolysis ($2H_2O \rightarrow O_2 + 2H_2$) provides a potential pathway for the production of clean,

Journal Name

ARTICLE

Table 1. Comparison studies for various LDHs-based materials and their SCs performances

Materials	Specific Capacitance ($F\ g^{-1}$)	Rate Capability: Retention	Stability: Retention (Cycle numbers)	Energy Density: ($Wh\ kg^{-1}$)	Power Density: ($kW\ kg^{-1}$)	References
CoAl-LDH	145 (2 A g^{-1})	/	/	/	/	Ref. 99
CoAl-LDH/rGO	1031 (1 A g^{-1})	24.2% (20 A g^{-1})	100% (6000)	/	/	Ref. 79
CoAl-LDH/MnO_2/Carbon fibers	944 (1 A g^{-1})	64.6% (20 A g^{-1})	98.2% (6000)	/	/	Ref. 103
CoAl-LDH/Ni foam	930 (2 A g^{-1})	71.9% (16 A g^{-1})	88.9% (2000)	/	/	Ref. 104
CoAl-LDH@PEDOT	672 (1 A g^{-1})	63.1% (40 A g^{-1})	92.5% (5000)	39.4	/	Ref. 33
NiAl-LDH Microspheres	735 (2 A g^{-1})	75% (25 A g^{-1})	116.5% (1000)	/	/	Ref. 66
NiAl-LDH/rGO	1255.8 (1 A g^{-1})	755.6 (6 A g^{-1})	106% (1500)	/	/	Ref. 105
GSP-LDH	1043 (1 A g^{-1})	87.5% (20 A g^{-1})	84% (2000)	20.4	9.3	Ref. 69
NiAl-LDH/Ni foam	701 (10 mA cm^{-2})	57.2% (40 mA cm^{-2})	94% (400)	/	/	Ref. 106
NiAl-LDH@Carbon nanoparticles	1146 (2 mV s^{-1})	42% (200 mV s^{-1})	88.9% (2000)	47.7	51	Ref. 107
NiCoAl-LDH/Graphite paper	1297 (1 A g^{-1})	59% (30 A g^{-1})	97% (10000)	58.9	14.9	Ref. 108
MnNi-LDH/Carbon nanotubes	2960 (1.5 A g^{-1})	79.5% (30 A g^{-1})	99.1% (2000)	88.3	17.2	Ref. 35
NiCo-LDH@CNT/nickel foam (NF)	2046 (1 A g^{-1})	65.2% (15 A g^{-1})	78% (1200)	89.7	8.7	Ref. 72
MnCo-LDH/Carbon fibers	1079 (2.1 A g^{-1})	82.5% (42 A g^{-1})	96.3% (6000)	126.1	109.8	Ref. 101
CoNiAl-LDH/Carbon black	501 (10 A g^{-1})	47% (10 A g^{-1})	91% (1000)	/	/	Ref. 109
CoNi-LDH/Graphene	650 (5 A g^{-1})	76.9% (30 A g^{-1})	97% (2000)	/	/	Ref. 110
CoNi-LDH/Ni foam	2682 (3 A g^{-1})	63.6% (20 A g^{-1})	82% (5000)	188	5.6	Ref. 34
CoNi-LDH/ PEDOT:PSS	960 (2 A g^{-1})	83.7% (30 A g^{-1})	93% (1000)	46.1	/	Ref. 59
PPy@CoNi-LDH	2342 (1 A g^{-1})	66.2% (20 A g^{-1})	115.4% (20000)	46	12	Ref. 97

renewable H_2 fuel for fuel cells and other energy devices.[119–122] However, the efficiency of water electrolysis is limited by high kinetic overpotential and sluggish reaction rate which has become the bottleneck for the further development of these energy-related devices. Although IrO_2 and RuO_2 have shown satisfactory electrocatalytic property in acidic and alkaline environment respectively, the scarcity, high cost and low stability of the noble metal-based catalysts hinder their practical applications.[123,124] Therefore, the development of efficient water electrolysis catalysts with earth-abundant elements and excellent stability has inspired years of research.

LDHs-based materials containing transition metal cations, particularly Ni, Co, Fe and Zn-containing LDHs, have been widely used in electrocatalytic reactions, especially for oxygen evolution reaction (OER).[45,46,58,80,125–144] Table 2 summarizes the recent developed LDHs-based OER catalysts and their electrochemical performances. Typically, Hu *et al.*[126] obtained single-layer nanosheet of NiFe-, NiCo- and CoCo-LDH successfully with a liquid phase exfoliation. The exfoliated LDHs nanosheets show a significantly higher catalytic activit and better stability (~95% at 10 mA cm^{-2} for 12 h) compare with their bulk phase, which is attributed to the increase o active site density and conductivity. It was found that NiFe-LDH nanosheets possess the best OER property (with a overpotential of ~290 mV in 1 M KOH at a current density o 10 mA cm^{-2}). Boettcher *et al.*[130] further discussed the active sites of NiFe-LDH. They demonstrated that Fe affects the loc electronic structure of the NiOOH and may serve as the active site. Up to now, various LDHs, such as CoFe-, CoNi-, ZnCo- and ZnNi-LDH, have been reported as OER catalysts. For exam le, compared with traditional monometallic $Co(OH)_2$ and Co_3O_4 systems, ZnCo-LDH possesses a lower overpotential (by ~10 mV) for the electrochemical oxidation of water, and i s turnover frequency (TOF) is 10 times larger than that o $Co(OH)_2$ and Co_3O_4 at the same applied potential.[141] In addition to the composition, the nanostructure o electroactive species also plays an important role in improvin the electrocatalytic performance. For instance, our gr

successfully fabricated NiFe-, CoFe- and LiFe-LDH arrays with a 3D architecture by a fast electrosynthesis method.[46] Compared with the conventional 2D planar architecture, the as-obtained NiFe-LDH array possesses a much lower onset potential (~1.43 V *vs*. RHE), larger current density (44 mA cm^{-1} at an overpotential of 300 mV) and superior stability (~100% at 1.55–1.75 V for 50 h).

Carbon-based materials, such as carbon nanotubes (CNTs), graphene and carbon quantum dots (CQDs) have been widely used as catalyst supports in many heterogeneous reactions, due to their high specific surface areas, satisfactory mechanical strength, thermal stability and electronic conductivity. Incorporating carbon-based materials and LDHs into nanocomposites for high performance OER catalysts has attracted increasing interest. Dai and co-works reported a NiFe–LDH/CNT hybrid which was assembled by direct nucleation and growth of ultrathin NiFe-LDH nanoplates on mildly oxidized multiwalled carbon nanotubes.[125] The resulting NiFe-LDH/CNTs material exhibits excellent electrocatalytic activity for oxygen evolution: in 1 M KOH, the OER onset potential decreases considerably to ~1.45 V *vs* RHE; and the tafel slope is 31 mV dec^{-1}, much smaller than that of Ir/C reference sample. The NiFe-LDH/CNT catalyst shows a nearly constant operating potential when testing at 5 mA cm^{-2}. As a zero band gap semiconductor carbon-based material, graphene has been extensively investigated as a substrate to anchor LDH for efficient OER catalysts. For example, Long *et al.*[58] reported an OER hybrid catalyst by alternately stacking the NiFe double hydroxide cation layers with the negatively-charged GO layers, and the as-prepared NiFe-LDH/GO and NiFe-LDH/rGO hybrids exhibited advanced electrocatalytic activity and stability toward OER in alkaline solution. The overpotential of catalytic OER is among the lowest values of non-noble metal catalysts (as low as 0.195 V) and the Tafel slope is close to the Ir/C catalyst (40 mV dec^{-1}). Recently, a novel composite based on NiFe-LDH and nitrogen-doped graphene (N-graphene) framework by spatially confined hybridization has been reported.[80] The superior OER catalytic performances, as evidenced by a remarkably decreased overpotential (~337 mV required for 10 mA cm^{-2}), a low Tafel slope (ca. 45 mV dec^{-1}) and long-term stability, indicate that the proposed NiFe-LDH/N-graphene was favorable for superior electrocatalysis. In addition, NiFe-LDH combined with carbon quantum dots (denoted as NiFe-LDH/CQD) has also been reported with enhanced OER activity.

Photoelectrochemical (PEC) water splitting into hydrogen and oxygen by the direct use of sunlight is an ideal, renewable method of clean energy production that integrates solar energy collection and water electrolysis into a single photoelectrode. LDHs materials have been employed to improve the photocurrent of PEC electrodes by facilitating electron-hole pair separation and improving O_2 evolution kinetics. Our group fabricated well-aligned ZnO core@LDH shell hierarchical nanoarrays by direct deposition of LDH nanosheets onto ZnO nanowires (NWs) *via* a facile electrosynthesis method.[66] The as-obtained ZnO@CoNi-LDH core–shell nanoarray exhibits promising behavior in PEC water splitting, giving rise to a largely enhanced photocurrent densi and stability, much superior to those of ZnO-base photoelectrodes.

As core process of direct alcohol fuel cells (DAFC), gluc biofuel cells (GBFC) and bio-sensors, small molecules electr oxidation reactions (e.g., methanol, ethanol, hydrazine and glucose), have attracted considerable attention. However, th anodic electro-oxidation process is normally greatly constrained by high kinetic barrier (high overpotentials sluggish reaction dynamics and instability of electrode materials. Even with the presence of state-of-the-art precious catalysts (such as Pt, Pd and Au), a substantial overpotential is still required to drive the oxidation of small molecules.[145,14 Moreover, noble catalysts also suffer from their high cost an easy toxication. Recently, great efforts have been focused o the oxides/hydroxides of first-row transition metals a promising electro-oxidation catalysts. Attributed to th intrinsically high catalytic activity of the transition metals in the hydroxide layers of LDHs, they have been directly use promising small molecules electrocatalysts. For instance, the hierarchical NiAl-LDH microspheres present a significant electrocatalytic performance toward the oxidation of hydrazine with a linear response range (5.0×10^{-6} –1.0×10^{-4} M) and high sensitivity (144 μA/μM cm^2).[147] The hierarchic MgFe-LDH microspheres with tunable interior architectures (hollow, yolk-shell and solid interior structure) were further explored.[148] The hollow MgFe-LDH microspheres displa excellent catalytic activity and robust durability for ethanol electrooxidation compared with the yolk-shell and soli structure, which can be ascribed to the enhanced surface are and suitable mesopore distribution. In addition, 3D NiFe-LD nanoarrays synthesized by an electrochemical method als show good electrocatalytic activity for hydrazine, methano and ethanol.[46]

By virtue of the confined effect of the interlayer and external surface of LDHs, LDHs can serve as efficient supports to anchor and disperse novel metal nanoparticles (Pt, Pd and Au, *etc*) or organic molecules for electrocatalysis. Our group reported a hierarchical Pd-based heteronanostructure wit finely-dispersed Pd nanoparticles (NPs) anchoring to vertically aligned LDH-NWs by using an *in situ* spontaneous depositio route.[149] The resulting Pd/LDH-NW heteronanostructur exhibits an excellent catalytic activity and robust durability fo ethanol electrooxidation. A combined DFT calculation an positron annihilation study indicate that the LDH support stabilizes the Pd NPs *via* the formation of a Pd–OH bond, an the redistribution of charge density (electron transfer from LDH to Pd NPs) further facilitates the process of ethanol electro-oxidation. We further reported the fabrication of glucose electrochemical sensor by alternating assembly of exfoliated LDH nanosheets and Au NPs on conductin substrates by using the LBL approach.[57] The as-fabricated electrode displays remarkable electrocatalytic performance toward the oxidation of glucose with high sensitivity, lo detection limit as well as long-term stability. The results demonstrate that LDH nanosheets serve as promising materials for the immobilization of metal particles, which can

Journal Name

ARTICLE

Table 2. Comparison studies for various LDHs-based materials and their OER activity

Materials	Electrolyte	Onset Potential (V vs. RHE)	η at J=10 mA cm^{-2} (mV)	J at η=300 mV (mA cm^{-2})	Tafel Slope (mV dec^{-1})	Stability	References
NiFe-LDH array	1 M KOH	1.46	230	40	50	10 h at 1.5V (~97%)	Ref. 127
Exfoliated NiFe-LDH nanosheet	1 M KOH	1.53	290	9	40	12 h at 10 mA cm^{-2} (~95%)	Ref. 126
NiFe-LDH particle	1 M KOH	1.43	260	/	/	/	Ref. 129
NiFe-LDH array	1 M KOH	1.46	/	/	/	12 h at 10 mA cm^{-2} (~99%)	Ref. 130
NiFe-LDH/Graphene particle	1 M KOH	1.44	205	/	39	1.5 h at 5 mA cm^{-2} (~99%)	Ref. 58
NiFe-LDH/Graphene/ Ni foam	0.1 M KOH	1.47	325	44	44	2.5 h at 10 mA cm^{-2} (~99%)	Ref. 128
nNiFe LDH/NGF	0.1 M KOH	/	337	45	45	10 h at 1.58V (~99%)	Ref. 80
$Ni_{2/3}Fe_{1/3}$-rGO	1 M KOH	/	210	40	42	10 h at 10 mA cm^{-2} (~97%)	Ref. 83
NiFe-LDH/CQD particle	1 M KOH	1.46	235	35	30	0.83 h at 2.5 mA cm^{-2} (~97%)	Ref. 76
NiFe-LDH/CNT particle	1 M KOH	1.45	240	45	31	0.28 h at 2.5 mA cm^{-2} (~100%)	Ref. 125
NiFe-LDH array	1 M KOH	1.43	224	44	52	50 h at 1.55–1.75 V (~100%)	Ref. 25
Flower-like Ni-Fe LDH	1 M KOH	1.446	344	/	97	11 h at 1.25 mA cm^{-2} (~98%)	Ref. 131
Ni-Fe/3D-ErGO	1 M KOH	/	259	/	39	2 h at 1.49 V (~90%)	Ref. 132
Mo intercalated NiFe-LDH	1 M KOH	1.47	280	/	40	6000s at 5 mA cm^{-2} (~100%)	Ref. 133
Ni_5Fe_1-LDH/RGO	1 M KOH	1.46	245	45	/	1000 cyclings at 1.10-1.85 V (~100%)	Ref. 134
$FeNi_8Co_2$ LDH nanosheets	1 M KOH	1.44	220	/	42	/	Ref. 135
NiCoFe LDH nanoarray	1 M KOH	/	/	150	53	10 h at 300 mA cm^{-2} (~90%)	Ref. 136
CoFe-LDH nanoparticles	1 M KOH	1.51	350	/	/	10000s at 1.58 V (~100%)	Ref. 137
CoNi-LDH nanoplates	1 M KOH	/	367	/	40	6 h at 10 mA cm^{-2} (~95%)	Ref. 138
CoNi-LDH array	0.1 M KOH	1.52	420	/	113	4000s at 1.52 V (~98%)	Ref. 139
NiZn-LDH nanocage	1 M KOH	1.43	290	/	43	10 h at 10 mA cm^{-2} (~99%)	Ref. 140
ZnCo-LDH nanoparticles	0.1 M KOH	1.57	500	/	/	10 h at 1.59 V (~100%)	Ref. 141
ZnCo-LDH sheets	0.1 M KOH	1.46	470	/	101	10 h at 1.55 V (~99%)	Ref. 142
ZnCo-LDH array	0.1 M KOH	1.56	490	/	83	1 h at 1.66 V (94%)	Ref. 45
CoMn-LDH nanoparticles	1 M KOH	/	323	/	43	3 h at 10 mA cm^{-2} (~90%)	Ref. 143

Journal Name

ARTICLE

be potentially applied in the fields of fuel cells and electrochemical sensors.

5. Conclusions and prospective

LDHs represent one of the most promising electrode materials due to their facile preparation/modification, good tunability and cost effectiveness. LDH-based eletroactive materials have been rationally designed and synthesized by well-developed methodologies with enhanced mass diffusion and electron transfer; a large number of methods have been established to directly modify electrode by using LDHs materials in order to give highly-dispersed and ordered nanostructures. The hierarchical LDHs microspheres with large surface area and suitable mesopore distribution facilitate the faradic redox reaction and the mass transfer of electrolytes, which thereby improves their electrochemical performances. Moreover, the LDHs/carbon (graphene, CNTs, carbon fiber or carbon clothes) nanocomposites fabricated by *in situ* growth of LDHs nanoplatelets on carbon materials or by assembly of LDHs with carbon counterparts can fully inherit the properties of both LDHs and carbon materials. In addition, some interesting nanostructures, such as carbon nanorings and graphene quantum dots, have been obtained by carbonization of interlayer anions of LDHs *via* the approach of confined synthesis. Besides carbon materials, LDHs/conducting polymer (CPs) composites also demonstrate a synergistic effect: the conducting polymers serve as the support for the dispersion of LDH nanoplatelets and provide satisfactory conductivity; while the electrochemically-active center in LDHs is excited extremely by virtue of the enhanced conductivity. Therefore, the LDHs-based electroactive materials obtained by rational design and controlled synthesis show significant potentials in the electrochemical energy storage and conversion.

The fabrication of hierarchical LDHs nanostructures and the construction of LDHs-based nanocomposites are effective routes for improving the electrochemical performances of LDHs. However, it remains a challenge to precisely manipulate the LDHs into arbitrary nanoarchitectures, in order to achieve an accurate tailoring of LDHs electronic structure and architecture on multi-scale levels; and detailed insights into the electrochemical reaction processes are not well-developed. Recently, LDHs materials have been proved with great opportunities as novel OER catalysts. However, new insights on their chemistry and physics are quite important to provide a general understanding for the catalytic reactions; and the relationship between the composition/structure and their properties needs to be revealed. Therefore, in the future, it is worthy to further design and synthesize low-cost and high-quality LDH-based electrodes with precise control ove composition, structure and morphology. Moreover, the understandings on the roles of active sites, the synergy between two or more active components of LDHs for th electron transportation and surface reaction are ver challenging and significant. In addition, the applicatio enhancement in the field of energy storage and conversion (e.g., supercapacitors and water splitting) would be welcom by fully making use of the redox reactions and intrinsically catalytic property of LDHs-based materials.

Acknowledgements

We would like to thank all the co-workers cited in the references below for their invaluable contributions to the work described here. This work was supported by the Nation l Natural Science Foundation of China (NSFC), the 973 Program (Grant No. 2014CB932102). M. Wei particularly appreciates the financial aid from the China National Funds fo Distinguished Young Scientists of the NSFC.

Notes and references

1 A. S. Arico, P. Bruce, B. Scrosati, J. M. Tarascon and W. V. Schalkwijk, *Nat. Mater.*, 2005, **4**, 366.
2 Y. Li, M. Gong, Y. Liang, J. Feng, J. E. Kim, H. Wang, G. Hong, Zhang and H. Dai, *Nat. Commun.*, 2013, **4**, 1085.
3 Y. Liang, Y. Li, H. Wang and H. Dai, *J. Am. Chem. Soc.*, 201 **135**, 2013.
4 A. Manthiram, A. V. Murugan, A. Sarkar and T. Muraliganth, *Energy Environ. Sci.*, 2008, **1**, 621.
5 D. R. Rolison, J. W. Long, J. C. Lytle, A. E. Fischer, C. P. Rhode T. M. McEvoy, M. E. Bourga and A. M. Lubers, *Chem. Soc Rev.*, 2009, **38**, 226.
6 S. L. Candelaria, Y. Shao, W. Zhou, X. Li, Jie Xiao, J. G. Zhang, Y. Wang, J. Liu, J. Li and G. Cao, *Nano Energy*, 2012, **1**, 195.
7 K. S. Novoselov, A. K. Geim, S. V. Morozov, D. Jiang, Y. Zhang S. V. Dubonos, I. V. Grigorieva and A. A. Firsov, *Science*, 2004 **306,** 666.
8 A. K. Gein and K. S. Novoselov, *Nat. Mater.*, 2007, **6**,183.
9 K. S. Novoselov, V. I. Fal'ko, L. Colombo, P. R. Gellert, M. G Schwab and K. Kim, *Nature*, 2012, **490**,192.
10 J. Q. Hu, Y. Bando, J. H. Zhan, Y. B. Li and T. Sekiguchi, *Appl. Phys. Lett.*, 2003, **83**, 4414.
11 R. Deng, X. Xie, M. Vendrell, Y. T. Chang and X. Liu, *J. Am. Chem. Soc.*, 2011, **133**, 20168.
12 M. R. Lukatskaya, O. Mashtalir, C. E. Ren, Y. Dall'Agnese, P Rozier, P. L. Taberna, M. Naguib, P. Simon, M. W. Barsoum and Y. Gogotsi, *Science*, 2013, **341**, 1502.
13 O. Mashtalir, M. Naguib, V. N. Mochalin, Y. Dall'Agnese, M Heon, M. W. Barsoum and Y. Gogotsi, *Nat. Commun.*, 2013, **4**, 1716.
14 M. Ghidiu, M. R. Lukatskaya, M. Zhao, Y. Gogotsi and M. W. Barsoum, *Nature*, 2014, **516**, 78.

15 Q. Wang, K. Kalantar-Zadeh, A. Kis, J. N. Coleman and M. S. Strano, *Nat. Nanotechnol.*, 2012, **7**, 699.
16 M. Chhowalla, H. S. Shin, G. Eda, L. Li, K. P. Loh and H. Zhang, *Nat. Chem.*, 2013, **5**, 263.
17 J. He, M. Wei, B. Li, Y. Kang, D. G. Evans and X. Duan, *Struct. Bond.*, 2005, **119**, 89.
18 M. Meyn, K. Beneke and G. Lagaly, *Inorg. Chem.*, 1990, **29**, 5201.
19 Y. Omomo, T. Sasaki, L. Zhou and M. Watanabe, *J. Am. Chem. Soc.*, 2003, **125**, 3568.
20 Q. Wang and D. O'Hare, *Chem. Rev.*, 2012, **112**, 4124.
21 B. Sels, D. D. Vos, M. Buntinx, F. Pierard, A. K. D. Mesmaeker, and P. Jacobs, *Nature*, 1999, **400**, 855.
22 G. Fan, F. Li, D. G. Evans and X. Duan, *Chem. Soc. Rev.*, 2014, **43**, 7040.
23 B. M. Choudary, S. Madhi, N. S. Chowdari, M. L. Kantam and B. Sreedhar, *J. Am. Chem. Soc.*, 2002, **124**, 14127.
24 F. Millange, R. I. Walton, L. Lei and D. O'Hare, *Chem. Mater.*, 2000, **12**, 1990.
25 R. R. Shan, L. G. Yan, K. Yang, Y. F. Hao and B. Du, *J. hazard. Mater.*, 2015, **299**, 42.
26 J. H. Choy, S. J. Choi, J. M. Oh and T. Park, *Appl. Clay Sci.*, 2007, **36**, 122.
27 R. Liang, R. Tian, L. Ma, L. Zhang, Y. Hu, J. Wang, M. Wei, D. Yan, D. G. Evans and X. Duan, *Adv. Funct. Mater.*, 2014, **24**, 3144.
28 J. Luo, J. H. Im, M. T. Mayer, M. Schreier, M. K. Nazeeruddin, N. G. Park, S. D. Tilley, H. J. Fan and M. Grätzel, *Science*, 2014, **345**, 1593.
29 F. Ning, M. Shao, C. Zhang, S. Xu, M. Wei and X. Duan, *Nano Energy*, 2014, **7**, 134.
30 N. Yulian, L. Ruiyi, L. Zaijun, F. Yinjun and L. Junkang, *Electrochim. Acta*, 2013, **94**, 360.
31 J. Jiang, J. Zhu, R. Ding, Y. Li, F. Wu, J. Liu and X. Huang, *J. Mater. Chem.*, 2011, **21**, 15969.
32 F. Zhang, L. Guo, S. Xu and R. Zhang, *Langmuir*, 2015, **31**, 6704.
33 J. Han, Y. Dou, J. Zhao, M. Wei, D. G. Evans and X. Duan, *Small*, 2013, **9**, 98.
34 H. Chen, L. Hu, M. Chen, Y. Yan and L. Wu, *Adv. Funct. Mater.*, 2014, **24**, 934.
35 J. Zhao, J. Chen, S. Xu, M. Shao, Q. Zhang, F. Wei, J. Ma, M. Wei, D. G. Evans and X. Duan, *Adv. Funct. Mater.*, 2014, **24**, 2938.
36 Z. Lu, W. Xu, W. Zhu, Q. Yang, X. Lei, J. Liu, Y. Li, X. Sun and X. Duan, *Chem. Commun.*, 2014, **50**, 6479.
37 X. Lu and C. Zhao, *Nat. Commun.*, 2015, **6**, 6616.
38 E. Scavetta, B. Ballarin, C. Corticelli, I. Gualandi, D. Tonelli, V. Prevot, C. Forano and C. Mousty, *J. Power Sources*, 2012, **201**, 360.
39 K. Nejati, K. Asadpour-Zeynali, Z. Rezvani and R. Peyghami, *Int. J. Electrochem. Sci.*, 2014, **9**, 5222.
40 I. Gualandi, M. Monti, E. Scavetta, D. Tonelli, V. Prevot and C. Mousty, *Electrochim. Acta*, 2015, **152**, 75.
41 E. Scavetta, B. Ballarin, M. Gazzano and D. Tonelli, *Electrochim. Acta*, 2009, **54**, 1027.
42 D. A. Corrigan and R. M. Bender, *J. Electrochem. Soc.*, 1989, **136**, 723.
43 M. S. Yarger, E. M. P. Steinmiller and K.-S. Choi, *Inorg. Chem.*, 2008, **47**, 5859.
44 V. Gupta, S. Gupta and N. Miura, *J. Power Sources*, 2008, **177**, 685.
45 Y. Li, L. Zhang, X. Xiang, D. Yan and F. Li, *J. Mater. Chem. A*, 2014, **2**, 13250.
46 Z. Li, M. Shao, H. An, Z. Wang, S. Xu, M. Wei, D. G. Evans and X. Duan, *Chem. Sci.*, 2015, DOI: 10.1039/c5sc02417j.
47 J. Han, D. Yan, W. Shi, J. Ma, H. Yan, M. Wei, D. G. Evans and X. Duan, *J. Phys. Chem. B*, 2010, **114**, 5678.
48 S. Huang, X. Cen, H. Peng, S. Guo, W. Wang and T. Liu, *J. Phys. Chem. B*, 2009, **113**, 15225.
49 D. Yan, J. Lu, M. Wei, J. Han, J. Ma, F. Li, D. G. Evans and X. Duan, *Angew. Chem. Int. Ed.*, 2009, **48**, 3073.
50 L. Li, R. Ma, Y. Ebina, K. Fukuda, K. Takada and T. Sasaki, *J. Am. Chem. Soc.*, 2007, **129**, 8000.
51 Z. Liu, R. Ma, M. Osada, N. Iyi, Y. Ebina, K. Takada and T. Sasaki, *J. Am. Chem. Soc.*, 2006, **128**, 4872.
52 M. Shao, J. Han, W. Shi, M. Wei and X. Duan, *Electrochem. Commun.*, 2010, **12**, 1077.
53 X. Kong, J. Zhao, J. Han, D. Zhang, M. Wei and X. Duan, *Electrochim. Acta*, 2011, **56**, 1123.
54 B. Zhang, S. Shi, W. Shi, Z. Sun, X. Kong, M. Wei and X. Duan, *Electrochim. Acta*, 2012, **67**, 133.
55 X. Kong, X. Rao, J. Han, M. Wei and X. Duan, *Biosens. Bioelectron.*, 2010, **26**, 549.
56 X. Dong, L. Wang, D. Wang, C. Li and J. Jin, *Langmuir*, 2012, **28**, 293.
57 J. Zhao, X. Kong, W. Shi, M. Shao, J. Han, M. Wei, D. G. Evans and X. Duan, *J. Mater. Chem.*, 2011, **21**, 13926.
58 X. Long, J. Li, S. Xiao, K. Yan, Z. Wang, H. Chen and S. Yang, *Angew. Chem. Int. Ed.*, 2014, **53**, 7584.
59 J. Zhao, S. Xu, K. Tschulik, R. G. Compton, M. Wei, D. O'Hare, D. G. Evans and X. Duan, *Adv. Funct. Mater.*, 2015, **25**, 2745.
60 L. Li, Y. Feng, Y. Li, W. Zhao and J. Shi, *Angew. Chem. Int. Ed.*, 2009, **48**, 5888.
61 J. W. Lee, J. M. Ko and J. Kim, *J. Phys. Chem. C*, 2011, **115**, 19445.
62 J. Zhou, S. Yang, J. Yua and Z. Shu, *J. Hazard. Mater.*, 2011, **192**, 1114.
63 M. Shao, F. Ning, Y. Zhao, J. Zhao, M. Wei, D. G. Evans and X. Duan, *Chem. Mater.*, 2012, **24**, 1192.
64 J. Xu, F. He, S. Gai, S. Zhang, L. Li and P. Yang, *Nanoscale*, 2014, **6**, 10887.
65 F. Zhang, Y. Zhang, C. Yue, R. Zhang and Y. Yang, *AIChE J.*, 2014, **60**, 4027.
66 M. Shao, F. Ning, J. Zhao, M. Wei, D. G. Evans and X. Duan, *Adv. Funct. Mater.*, 2014, **24**, 580.
67 D. Tang, Y. Han, W. Ji, S. Qiao, X. Zhou, R. Liu, X. Han, H. Huang, Y. Liu and Z. Kang, *Dalton Trans.*, 2014, **43**, 15119.
68 J. Xu, S. Gai, F. He, N. Niu, P. Gao, Y. Chen and P. Yang, *J. Mater. Chem. A*, 2014, **2**, 1022.
69 X. Wu, L. Jiang, C. Long, T. Wei and Z. Fan, *Adv. Funct. Mater.*, 2015, **25**, 1648.
70 M. Li, F. Liu, J.P. Cheng, J. Ying and X. B. Zhang, *J. Alloy Compd.*, 2015, **635**, 225.
71 B. Yang, Z. Yang, R. Wang and T. Wang, *Electrochim. Acta*, 2013, **111**, 581.
72 X. Li, J. Shen, W. Sun, X. Hong, R. Wang, X. Zhao and X. Yan, *J. Mater. Chem. A,* 2015, **3**, 13244.
73 H. Wang, X. Xiang and F. Li, *J. Mater. Chem.*, 2010, **20**, 3944.
74 J. Yang, C. Yu, X. Fan, Z. Ling, J. Qiu and Y. Gogotsi, *J. Mater. Chem. A*, 2013, **1**, 1963.
75 Y. Wang, Z. Wang, Y. Rui and M. Li, *Biosens. Bioelectron.*, 2015, **64**, 57.
76 D. Tang, J. Liu, X. Wu, R. Liu, X. Han, Y. Han, H. Huang, Y. Liu and Z. Kang, *ACS Appl. Mater. Interfaces*, 2014, **6**, 7918
77 L. Qu, Y. Liu, J. Baek and L. Dai, *ACS Nano*, 2010, **4**, 1321.
78 Z. Gao, J. Wang, Z. Li, W. Yang, B. Wang, M. Hou, Y. He, Q. Liu, T. Mann, P. Yang, M. Zhang and L. Liu, *Chem. Mater.*, 2011, **23**, 3509.
79 L. Zhang, X. Zhang, L. Shen, B. Gao, L. Hao, X. Lu, F. Zhang, L. Ding and C. Yuan, *J. Power Sources*, 2012, **199**, 395.
80 C. Tang, H. Wang, H. Wang, Q. Zhang, G. Tian, J. Nie and F. Wei, *Adv. Mater.*, 2015, **27**, 4516.
81 J. Xu, S. Gai, F. He, N. Niu, P. Gao, Y. Chen and P. Yang, *J. Mater. Chem. A*, 2014, **2**, 1022.

82 L. Wang, D. Wang, X. Y. Dong, Z. J. Zhang, X. F. Pei, X. J. Chen, B. Chen and J. Jin, *Chem. Commun.*, 2011, **47**, 3556.
83 W. Ma, R. Ma, C. Wang, J. Liang, X. Liu, K. Zhou and T. Sasaki, *ACS Nano*, 2015, **9**, 1977.
84 A. I. Khan and D. O'Hare, *J. Mater. Chem.*, 2002, **12**, 3191.
85 H. Nakayama, N. Wada and M. Tsuhako, *Int. J. Pharm.*, 2004, **269**, 469.
86 X. Guo, F. Zhang, D. G. Evansa and X. Duan, *Chem. Commun.*, 2010, **46**, 5197.
87 M. Zhao, Q. Zhang, J. Huang and F. Wei, *Adv. Funct. Mater.*, 2012, **22**, 675.
88 J. Sun, H. Liu, X. Chen, D. G. Evans, W. Yang and X. Duan, *Adv. Mater.*, 2013, **25**, 1125.
89 L. Song, J. Shi, J. Lu and C. Lu, *Chem. Sci.*, 2015, **6**, 4846.
90 X. Zhang, J. Zhang, W. Song and Z. Liu, *J. Phys. Chem. B*, 2006, **110**, 1158.
91 J. Huang, S. Virji, B. H. Weiller and R. B. Kaner, *J. Am. Chem. Soc.*, 2003, **125**, 314.
92 A. M. Nardes, M. Kemerink, R. A. J. Janssen, J. A. M. Bastiaansen, N. M. M. Kiggen, B. M. W. Langeveld, A. J. J. M. van Breemen and M. M. de Kok, *Adv. Mater.*, 2007, **19**, 1196.
93 B. Kutlu, A. Leuteritz, R. Boldt, D. Jehnichen, U. Wagenknecht and G. Heinrich, *Appl. Clay Sci.*, 2013, **72**, 91.
94 D. M. Xu, M. Y. Guan, Q. H. Xu and Y. Guo, *J. Hazard. Mater.*, 2013, **262**, 64.
95 G. A. Snook, P. Kao and A. S. Best, *J. Power Sources*, 2011, **196**, 1.
96 G. Wang, L. Zhang and J. Zhang, *Chem. Soc. Rev.*, 2012, **41**, 797.
97 M. Shao, Z. Li, R. Zhang, F. Ning, M. Wei, D. G. Evans and X. Duan, *Small*, 2015, **11**, 3529.
98 B. E. Conway, V. Birss and J. Wojtowicz, *J. Power Sources*, 1997, **66**, 1.
99 L. Su and X. Zhang, *J. Power Sources*, 2007, **172**, 999.
100 M. Shao, F. Ning, Y. Zhao, J. Zhao, M. Wei, D. G. Evans and X. Duan, *Chem. Mater.*, 2012, **24**, 1192.
101 J. Zhao, J. Chen, S. Xu, M. Shao, D. Yan, M. Wei, D. G. Evans and X. Duan, *J. Mater. Chem. A*, 2013, **1**, 8836.
102 R. Ma, X. Liu, J. Liang , Y. Bando and T. Sasaki, *Adv. Mater.*, 2014, **26**, 4173.
103 J. Zhao, Z. Lu, M. Shao, D. Yan, M. Wei, D. G. Evans and X. Duan, *RSC Adv.*, 2013, **3**, 1045.
104 G. Pan, X. Xia, J. Luo, F. Cao, Z. Yang and H. Fan, *Appl. Clay Sci.*, 2014, **102**, 28.
105 L. Zhang, J. Wang, J. Zhu, X. Zhang, K. S. Hui and K. N. Hui, *J. Mater. Chem. A*, 2013, **1**, 9046.
106 J. Wang, Y. Song, Z. Li, Q. Liu, J. Zhou, X. Jing, M. Zhang and Z. Jiang, *Energy Fuels*, 2010, **24**, 6463.
107 X. Liu, C. Wang, Y. Dou, A. Zhou, T. Pan, J. Han and M.Wei, *J. Mater. Chem. A*, 2014, **2**, 1682.
108 J. Yang, C. Yu, X. Fan and J. Qiu, *Adv. Energy Mater.*, 2014, **4**, 1400761.
109 C. Yu, J. Yang, C. Zhao, X. Fan, G. Wang and J. Qiu, *Nanoscale*, 2014, **6**, 3097.
110 R. Ma, X. Liu, J. Liang , Y. Bando and T. Sasaki, *Adv. Mater.*, 2014, **26**, 4173.
111 M. S. Whittingham, *Chem. Rev.*, 2004, **104**, 4271.
112 P. Simon and Y. Gogotsi, *Nat. Mater.*, 2008, **7**, 845.
113 B. Kang and G. Ceder, *Nature*, 2009, **458**, 190.
114 X. Li, W. Yang, F. Li, D.G. Evans and X. Duan, *J. Phys. Chem. Solids*, 2006, **67**, 1286.
115 J. Jiang, J. Zhu, R. Ding, Y. Li, F. Wu, J. Liu and X. Huang, *J. Mater. Chem.*, 2011, **21**, 15969.
116 M. Zhao, Q. Zhang, J. Huang, G. Tian, J. Nie, H. Peng and F. Wei, *Nat. Commun.*, 2014, **5**, 3410.
117 J. Shi, H. Peng, L. Zhu, W. Zhu and Q. Zhang, *Carbon*, 2015, **92**, 96.
118 X. Cheng, G. Tian, X. Liu, J. Nie, M. Zhao, J. Huang, W. Z[illegible], L. Hu, Q. Zhang and F. Wei, *Carbon*, 2013, **62**, 393.
119 F. Cheng and J. Chen, *Nat. Chem.*, 2012, **4**, 962.
120 N. M. Markovic, *Nat. Chem.*, 2013, **12**, 101.
121 S. Y. Reece, J. A. Hamel, K. Sung, T. D. Jarvi, A. J. Esswein, J. J. H. Pijpers and D. G. Nocera, *Science*, 2011, **334**, 645.
122 T. Reier, M. Oezaslan and P. Strasser, *ACS Catal.*, 2012, **2**, 1765.
123 A. T. Marshall and R. G. Haverkamp, *Electrochim. Acta*, 2010, **55**, 1978.
124 Y. Lee, J. Suntivich, K. J. May, E. E. Perry and Y. Shao-Horn, *J. Phys. Chem. Lett.*, 2012, **3**, 399.
125 M. Gong, Y. Li, H. Wang, Y. Liang, J. Z. Wu, J. Zhou, J. Wang, T. Regier, F. Wei and H. J. Dai, *J. Am. Chem. Soc.*, 2013, **135**, 8452.
126 F. Song and X. Hu, *Nat. Commun.*, 2014, **5**, 4477.
127 Z. Lu, W. Xu, W. Zhu, X. Sun and X. Duan, *Chem. Commun.*, 2014, **50**, 6479.
128 H. F. Wang, C. Tang and Q. Zhang, *J. Mater. Chem. A*, 2015, **3**, 16183.
129 B. Hunter, J. Blakemore, M. Deimund, H. Gray and J. Winkler, *J. Am. Chem. Soc.*, 2014, **136**, 13118.
130 L. Trotochaud, S. Young, J. Ranney and S. Boettcher, *J. Am. Chem. Soc.*, 2014, **136**, 6744.
131 L. Zhou, X. Huang, H. Chen, P. Jin, G. Li and X. Zou, *Dalton Trans.*, 2015, **44**, 11592.
132 X. Yu, M. Zhang, W. Yuan and G. Shi, *J. Mater. Chem. A*, 2015, **3**, 6921.
133 N. Han, F. Zhao and Y. Li, *J. Mater. Chem. A*, 2015, **3**, 16348.
134 D. H. Youn, Y. B. Park, J. Y. Kim and G. Magesh, *J. Power Sources*, 2015, **294**, 437.
135 X. Long, S. Xiao, Z. Wang, X. Zheng and S. Yang, *Chem. Commun.*, 2015, **51**, 1120.
136 Q. Yang, T. Li, Z. Lu, X. Sun and J. Liu, *Nanoscale*, 2014, **6**, 11789.
137 G. Abellan, J. A. Carrasco, E. Coronado, J. Romero and M. Varela, *J. Mater. Chem. C*, 2014, **2**, 3723.
138 H. Liang, F. Meng, M. Acevedo, L. Li, A, Forticaux, L. Xiu, Z. Wang and S. Jin, *Nano Lett.*, 2015, **15**, 1421.
139 J. Jiang, A. Zhang, L. Li and L. Ai, *J. Power Sources*, 2015, **278**, 445.
140 S. Wang, J. Nai, S. Yang and L Guo, *ChemNanoMat.* 20[illegible], DOI: 10.1002/cnma.201500067.
141 X. Zou, A. Goswami and T. Asefa, *J. Am. Chem. Soc.*, 2013, **135**, 17242.
142 C. Qiao, Y. Zhang, Y. Zhu, C. Cao, X. Bao and J. Xu, *J. Mater. Chem. A*, 2015, **3**, 6878.
143 F. Song and X. Hu, *J. Am. Chem. Soc.*, 2014, **136**, 16481.
144 M. Gong and H. Dai, *Nano Res.*, 2015, **8**, 23.
145 M. K. Debe, *Nature*, 2012, **486**, 43.
146 C. Bianchini and P. K. Shen, *Chem. Rev.*, 2009, **109**, 4183.
147 X. Kong, J. Zhao, W. Shi, Y. Zhao, M, Shao and M. Wei, *Electrochim. Acta*, 2012, **80**, 257.
148 M. Shao, F. Ning, J. Zhao, M. Wei, D. G. Evans and X. Duan, *Adv. Funct. Mater.*, 2013, **23**, 3513.
149 J. Zhao, M. Shao, D. Yan, S. Zhang, Z. Lu, Z. Li, X. Cao, B. Wang, M. Wei, D. G. Evans and X. Duan, *J. Mater. Chem. A*, 2013, **1**, 5840.